PAN AIR Analysis of a Transport High-Lift Configuration

E. N. Tinoco,* D. N. Ball,† and F. A. Rice II‡
Boeing Commercial Airplane Company, Seattle, Washington

PAN AIR panel method analyses of 737-300 takeoff high-lift configurations were performed in support of the aircraft's flight development phase during a precertification flight test. The configurations analyzed feature a highly complex three-dimensional leading- and trailing-edge high-lift flap system. Modeling details of two takeoff flap settings consisting of significantly different flap and slat arrangements are presented. Computational results are presented and compared with flight test data. These comparisons include wing and nacelle pressure distributions, wing section lift coefficients, and aircraft L/D. The agreement of computational results with flight data is improved by incorporating in-flight aeroelastic twist and flap blow back. These improvements to the geometric description of the computational model were based on in-flight optical measurements and 737 structures load staff estimates.

Nomenclature

c = chord length based on cruise wing planform
C_D = drag coefficient
C_{Di} = induced drag coefficient
C_{Dp} = parasite drag coefficient
C_L = lift coefficient
C_l = section lift coefficient
C_p = pressure coefficient
$\bar{n}$ = unit normal vector
V_∞ = freestream velocity
V_{stall} = stall speed
$\bar{v}$ = perturbation velocity vector
$\bar{w}$ = perturbation mass flux vector
$\bar{W}$ = total mass flux vector
α = angle of attack
η = span fraction
σ = source strength
μ = double strength
ξ = vorticity strength
Φ = total potential
ϕ = perturbation potential

Subscripts

l = lower (or internal) side of panel
u = upper (or external) side of panel

Introduction

THE field of computational fluid dynamics (CFD) has made much progress in recent years, particularly in the area of three-dimensional transonic flows. Computational methods for the low-speed high-lift regime have emphasized the two-dimensional, viscosity dominated flowfield that exists near maximum lift. Three-dimensional high-lift modeling has been mainly limited to zero thickness inviscid lifting surface methods.[1-3] The area of full (thick) surface geometry modeling for high-lift configurations has not received much attention, probably because of the complexities of geometry definition as well as flowfield calculation.

During the spring of 1984, the Boeing 737-300 was well into flight testing in preparation for Federal Aviation Administration (FAA) certification. Modern onboard flight data computers, used during the precertification flight development phase, provided test results that indicated almost immediately whether the configuration being tested was an improvement.[4,5] Additional detailed data were desired to show why a test configuration was better or worse than previously flown configurations.

In an attempt to enhance the understanding and to provide guidance to the flight development program, two of the authors were called upon to support the flight test effort by means of a parallel computational effort. The decision to use the Boeing in-house version of the PAN AIR panel method code was made for several reasons: 1) The flight test configurations of interest had relatively low trailing-edge flap angles, thus reducing the influence of major viscous effects such as separation; 2) the flight regime being explored was conducted at speeds near to and greater than the 1.2 V_{stall} speed, hence there was no need to compute viscous flow near C_{Lmax}; 3) the data extraction capabilities of the program would provide both surface- and off-body flowfield parameters at any point; and 4) we were interested in whether or not a full three-dimensional high-lift configuration could be analyzed successfully. Previous attempts with PAN AIR had been limited to isolated wings with deployed leading-edge slats and trailing-edge flaps.[3]

Computational Method

PAN AIR[6-9] is a general three-dimensional boundary value problem panel method solver for the Prandtl-Glauert equation. This panel method is applicable to the analysis of inviscid linear flows over vehicles in subsonic or supersonic flight, surface and underwater marine vehicles, and for internal flows, such as those in wind tunnels or in ducts. Several features distinguish PAN AIR from other panel methods. The most important features are its higher order numerics (linear source and quadratic doublet variation on each panel), continuity of doublet strength, continuity of geometry, a very general user-specified boundary condition equation, a very robust full direct matrix solver, and the implementation of the Kutta condition. Many of these features were deemed necessary to analyze the complex high-lift configurations successfully. PAN AIR currently exists in several code forms (both pilot and production) for dissemination throughout the United States. In this paper, PAN AIR will refer to the technology embodied in version 3.0, and in the Boeing in-house enhanced pilot code. Previous versions of

Received May 19, 1986; presented as Paper 86-1811 at the AIAA 4th Applied Aerodynamics Conference, San Diego, CA, June 9-12, 1986; revision received Oct. 17, 1986.

*Principal Engineer. Associate Fellow AIAA.
†Specialist Engineer. Member AIAA.
‡Engineer.

these codes should be capable of reproducing most of the results presented in this paper.

Configuration Geometry and Modeling

The 737-300, shown in Fig. 1, is a derivative of the 737-200 airplane. The major configuration changes are 1) forward body stretched 44 in., aft body stretched 60 in.; 2) wingspan extended 28 in.; 3) CFM56-3 engine and strut; 4) leading-edge slat contour change and chord length extension; 5) trailing-edge flap modifications (called thrust gates) or flipper flaps) to accommodate the strut and engine exhaust plume; 6) Krueger flap planform and contour change; 7) horizontal tail span extended 72 in.; and 8) dorsal extension to vertical tail.

The first six items were incorporated into the computational models. The horizontal and vertical tails were not incorporated into the analysis because their influence on the wing flowfield is minimal. The configurations of interest consisted of two takeoff flap settings, with flaps 15 used for most takeoffs, and flaps 1 used for high-altitude hot fields. The numerical designation refers to the nominal deflection angle of the trailing-edge flaps. The computational models consisted of approximately 1750 panels for the flaps 1 configuration, 2500 panels for the flaps 1 configuration inside a wind tunnel, and up to 2900 panels for the flaps 15 models. A flaps 15 paneling is shown in Fig. 2. The body and nacelle paneling were based upon previous work by the 737-300 configuration staff. The wing, leading- and trailing-edge devices, and related wake panelings were developed specifically for this study.

The leading-edge devices consisted of an inboard Krueger flap and an outboard slat. The Krueger flap contours were not yet finalized at the time this study was conducted, so the initial rollout Krueger flap configuration was used. The Krueger had a single deployed position requiring a rotation of 96 deg from the wing's lower surface. As a modeling simplification, the Krueger was represented by a thin doublet sheet and translated slightly from its true position to provide a convenient abutment between the wing leading edge and the Krueger trailing edge (Fig. 3). This abutment was a requirement of the mathematical conditions applied at network edges to insure doublet strength continuity; because the Krueger trailing edge was abuted to the wing, it was not necessary to shed a wake from the Krueger flap.

Two outboard slat configurations were modeled. The 17-deg rotation position, used with low-trailing edge flap angles, is sealed against the wing. For this slat position, the slat geometry was integrated into the wing paneling as illustrated in Fig. 4. This modeling was used for the flaps 1 configuration. The 30-deg slat position, used with the higher trailing-edge flap angles, had a gap between the wing and slat. Here the slat was treated as a separate element entirely. The wing leading edge was repaneled to represent the fixed portion of the wing beneath the slat. The shed vorticity from the slat was carried downstream by a wake doublet sheet running parallel to and above the wing upper surface as shown in Fig. 5. The distance between the vorticity sheet and wing was equal to the gap between the slat trailing edge and the wing. Previous PAN AIR studies had shown that solutions were not very sensitive to the exact position of the slat trailing wake. This modeling was used in the representation of the flaps 15 configuration.

Modeling the trailing-edge flaps also required special considerations. The flaps 1 (1 deg) takeoff flap deflection angle was paneled as an integral part of the wing. This was accomplished by moving the triple slotted flaps to the correct positions and then picking discreet points that would best describe the merged geometry as illustrated in Fig. 4. Although the resulting wing sections with the sealed leading-edge slat and merged trailing-edge flaps are smooth in the chordwise direction, the planform geometry still has several spanwise discontinuities as shown in Fig. 6. The spanwise

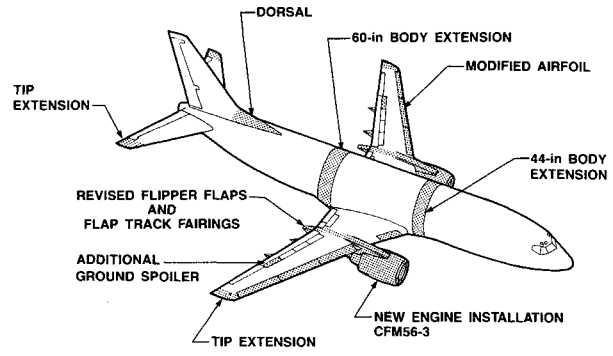

Fig. 1 737-300 comparison to the 737-200.

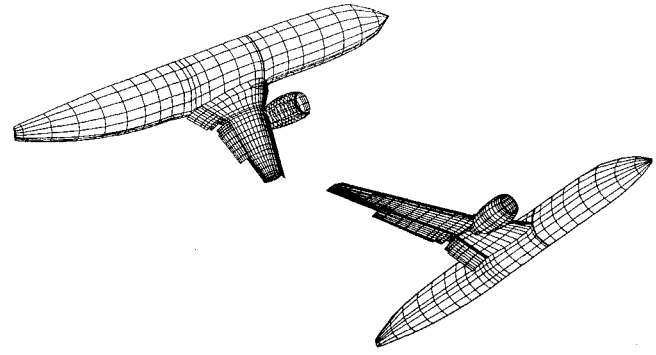

Fig. 2 Paneling—flaps 15 configuration.

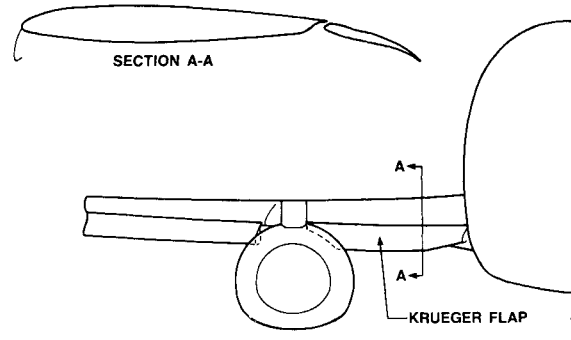

Fig. 3 Krueger flap.

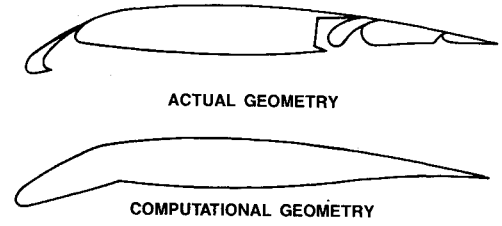

Fig. 4 Merged flaps 1 geometry—wing section.

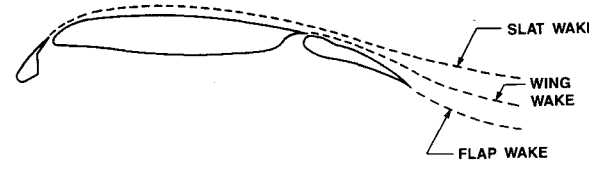

Fig. 5 Flaps 15 geometry and wakes.

discontinuities at the end of the deflected leading-edge slat were sealed with side edge paneling that resulted in a 0.1-in. gap (full scale) between opposing sides. The trailing-edge discontinuities between the thrust gates and flaps were filled with very small triangular networks to give a continuous edge from which to shed the trailing wake. These gap filling panels were treated as an impermeable addition to the wing surface. Neither the close opposition of adjacent panels, nor the proximity of panels of greatly differing area required any special panel sequence ordering or resulted in any numerical difficulties.

The larger 15-deg flap deflection for the flaps 15 cases was handled by paneling the triple slotted flaps as a single element separate from the wing. At this flap setting the gap between the forward vane and the main flap has not yet opened, and the gap between the main and aft flap is still minimally opened. A comparison of the true and modeled geometries is shown in Fig. 7. The relation between the wakes from the slat, wing, and trailing flap are illustrated in Fig. 5. The wing wake extends from wing tip to the side of the body with abutments between all adjacent wake networks that made up the wake shed from the wing trailing edge. The flap and slat wakes extend only the width of the elements from which they were shed. The resulting wing planform, without leading- and trailing-edge flaps, also has several leading- and trailing-edge spanwise discontinuities that were paneled closed as shown in Fig. 8.

The nacelle modeling was based on previous work.[10] Initially, a solid exhaust plume model was used. Later studies included use of a more complex model shown in Fig. 9. This model included a more realistic simulation of the exhaust geometry and its effects. A network at midlength of the interior of the fan cowl is used both to control the mass flow into the inlet and provide an exhaust through the fan duct over the core cowl. This network provided the only connection between the fan cowl and the core cowl. The specification of zero total potential over the backside of this control network and on the base of the core cowl ensures a well-posed boundary-value problem for the exhaust simulation. Wake-type plumes were shed from the trailing edge of the fan cowl and the base of the core cowl. No significant differences have been noted between the two nacelle simulations, although the latter is deemed to be a more realistic representation. The nacelle was attached to the wing with a simple thin-doublet-sheet strut. The nacelle paneling was rather sparse in that the main interest was on the wing flow.

To account for the twist effects of aerodynamic loading on the wing, the entire wing model was twisted about the wing's elastic axis as a function of wing span location. The twist distribution was based on preflight estimates provided by the 737 Structures Load staff and was modified on the basis of in-flight measurements taken at two spanwise locations. Also taken into account was the amount of flap rotation due to

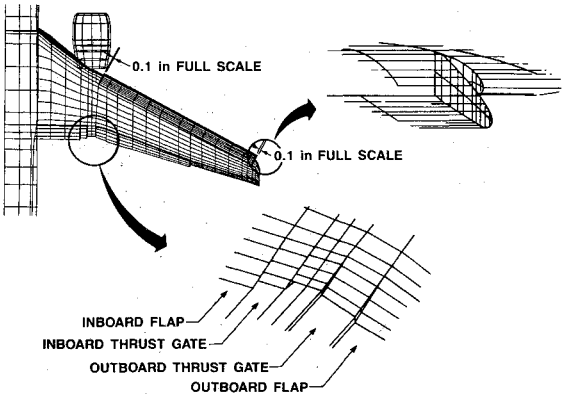

Fig. 6 Merged flaps 1 geometry—wing planform.

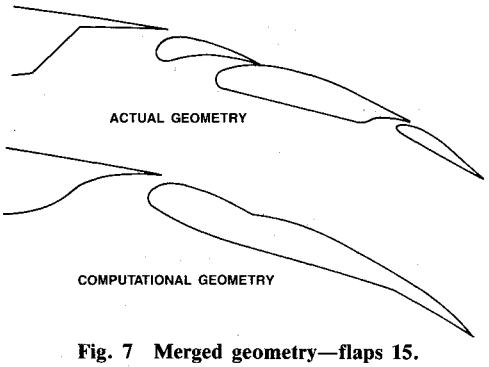

Fig. 7 Merged geometry—flaps 15.

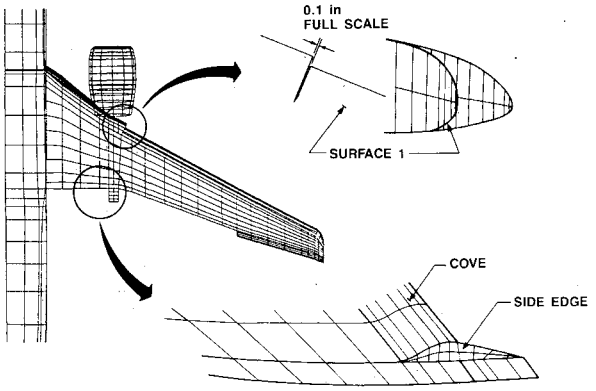

Fig. 8 Side-edge paneling—flaps 15.

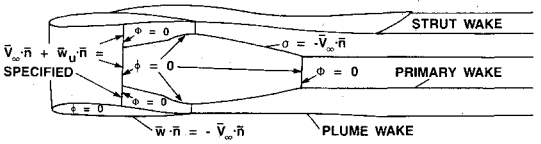

Fig. 9 Nacelle modeling.

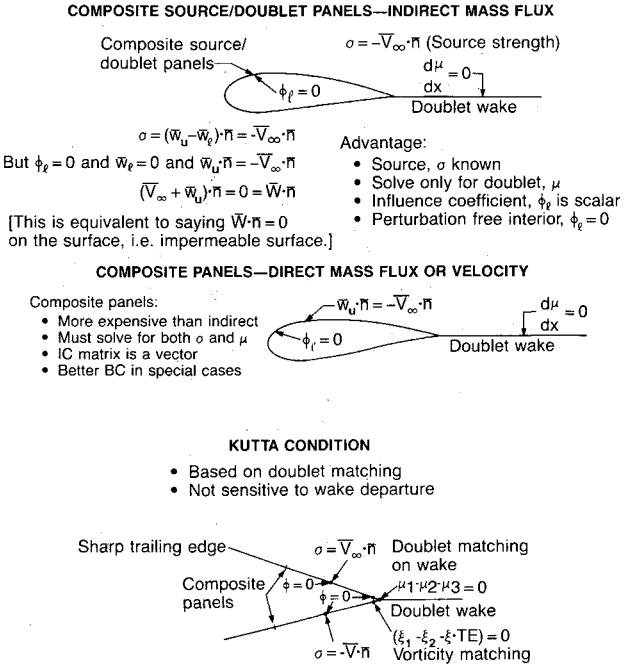

Fig. 10 Boundary and Kutta conditions.

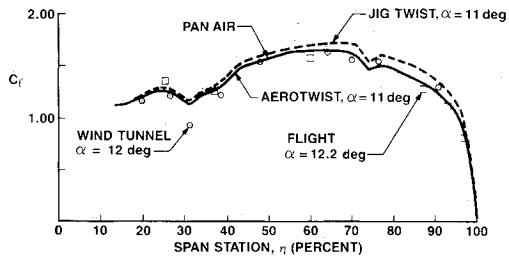

Fig. 11 737-300 flaps 1 wing spanload.

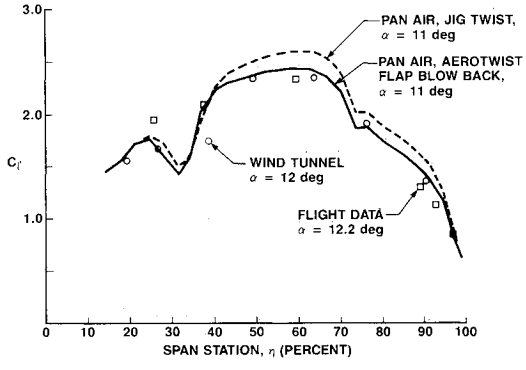

Fig. 12 737-300 flaps 15 wing spanload.

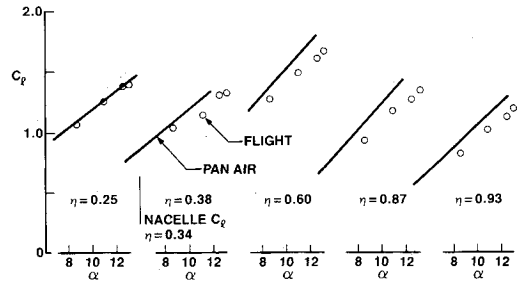

Fig. 13 Flaps 1 section lift.

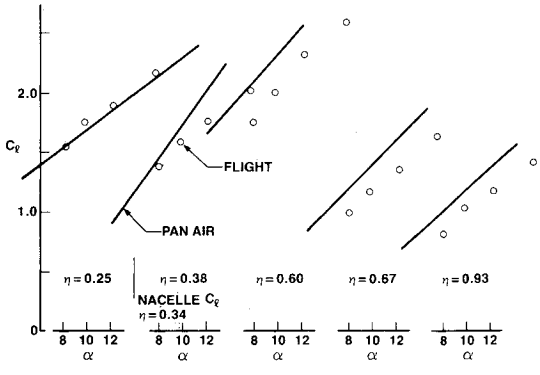

Fig. 14 Flaps 15 section lift.

load on the flaps 15 configuration. Ground tests and in-flight photographs showed that the outboard flaps would decrease as much as 2–3 deg in deflection angle when deployed in flight. This is a result of the load reversal on the tracks and rollers used in the actuation system. During ground rigging, the weight of the flaps pulls the system down; in-flight, the aerodynamic loads work in the opposite direction.

Unless otherwise stated, composite source and doublet panels were used to represent the geometry with indirect mass flux impermeability boundary conditions. On the nacelle, the leading-edge slat, and the trailing-edge flaps in the flaps 15 configuration, the more robust direct mass flux impermeability boundary condition was used. The vorticity-matching Kutta condition available in PAN AIR version 3.0 and in the Boeing in-house enhanced pilot code was used on all sharp trailing edges. These boundary conditions are illustrated in Fig. 10. Previous studies have shown that the vorticity-matching Kutta condition is more robust than the doublet-matching condition originally in PAN AIR. No attempts were made to determine if the doublet-matching Kutta condition would have been adequate for this analysis. Together, the more expensive direct impermeability specification used where appropriate (a judgment call) along with the vorticity-matching Kutta condition, produce robust and reliable solutions even with unusual or sparse paneling.

Results

The PAN AIR analysis was carried out concurrently with the precertification flight-test development. Eighteen major cases were analyzed during a three-month period. These cases included the basic flaps 1 and flaps 15 configurations with wind tunnel or flight twist, flow-through and powered nacelles, free-air and in-the-wind-tunnel solutions; ground effect, sealed and slotted slats; and other geometric variations. Comparisons of some of these PAN AIR results were made with experimental data obtained during the precertification development phase of flight test on the 737-300. Surface pressure distributions on the wing and the nacelle of the aircraft were obtained during a series of flights. Plastic tubing was bonded to the wing surface at six spanwise locations and to one nacelle at eight circumferential locations. For the takeoff configurations, the flaps and leading edge slat were fixed for the entire flight with the plastic pressure tubing draped over their surfaces. Pressure data were taken for a series of fixed conditions in terms of percentage of stall speed. Data were obtained for a nominal 1.4, 1.3, 1.2, and 1.1 times stall speed for the aircraft weight and altitude. During another flight at similar loading conditions, measurements were made with optical targets on the wing that combined with twist estimates provided by the 737 Structures Load staff and allowed a nominal definition of the aeroelastic twist of the wing to be determined. This twist distribution was then incorporated in the PAN AIR computational models.

The flight pressure measurements at each spanwise location were integrated to yield a section lift coefficient for each flight condition. These data were then compared with PAN AIR results. Fig. 11 shows a comparison of spanwise lift distribution for the flaps 1 configuration. Flight and wind tunnel data as well as PAN AIR results for both jig and aeroelastic wing-twist distributions are presented. The comparisons were made for comparable lift conditions. The low-speed wind-tunnel model, originally built in the late 1960s during the 737-100/200 development and later modified to the 737-300 configuration, featured the jig twist. The inclusion of the aeroelastic twist in the computational model is necessary for good test-theory agreement with flight. Fig. 12 shows a similar comparison for the flaps 15 configuration. Here, in addition to the inclusion of the aeroelastic twist, it was also necessary to account for the flexibility of the outboard flap tracks in the flaps 15 position. A nominal estimate of this deflection or "blowback" was incorporated into the PAN AIR models. Good agreement has also been found between PAN AIR estimates and wing spanwise lift distributions extracted from wind tunnel wake surveys.[11]

Figures 13 and 14 show the variation of local wing lift coefficient with angle of attack for the flaps 1 and flaps 15 configurations. The flight test data show the wing to be operating in the linear range of lift coefficient even at these high angles of attack. The PAN AIR results are in good agreement with the flight data. The overprediction of lift

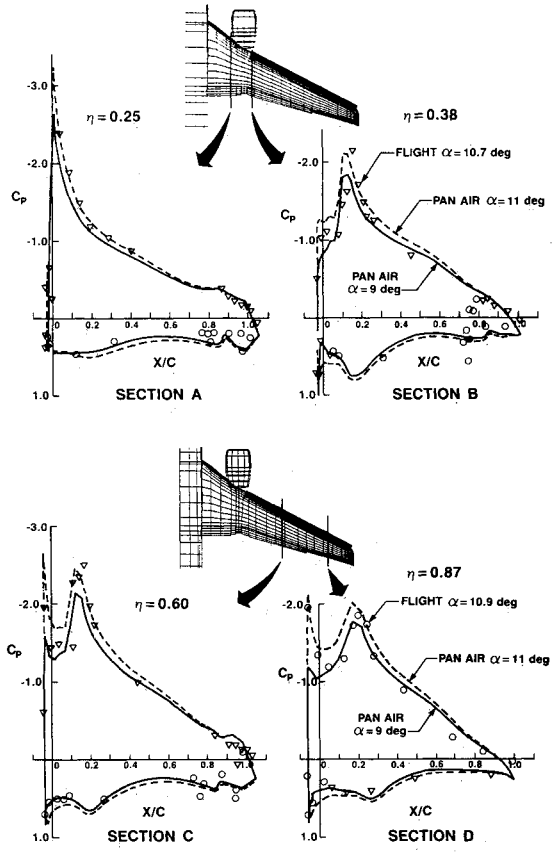

Fig. 15 Flaps 1 wing pressure distribution.

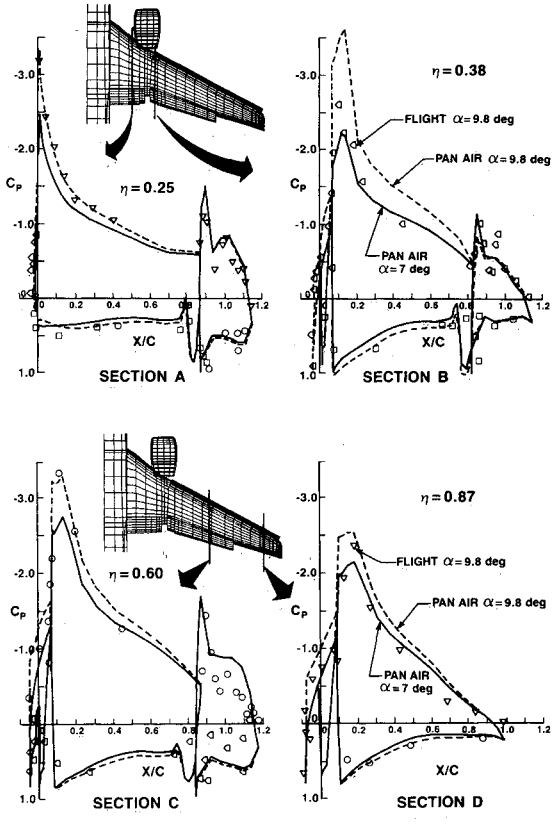

Fig. 16 Flaps 15 wing pressure distribution.

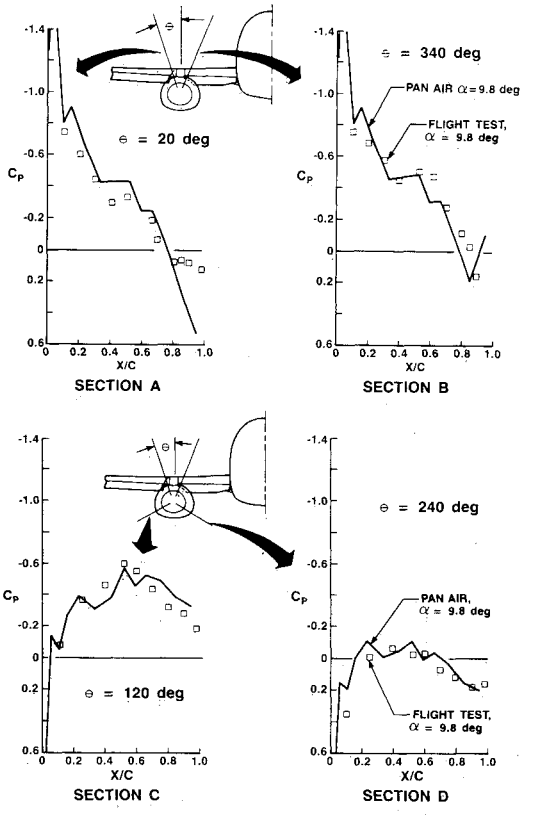

Fig. 17 Nacelle pressure distribution.

level and slope on the outboard sections are to be expected due to the lack of any viscous modeling in the PAN AIR calculations.

Detailed streamwise pressure distribution comparisons were made between the flight data and the computational results. Comparisons for the flaps 1 configuration are shown in Fig. 15. PAN AIR results are shown for both an approximate angle of attack match and for a lift match. Considering the many factors influencing this comparison, such as flap blowback, aeroelastic effects, and neglect of viscous effects in PAN AIR, the agreement was surprisingly good. The simplifications made to the computational geometry to simulate the sealed slat geometry did not unduly compromise the results. The sealed slat pressures were very well predicted, as were the overall pressure distributions. Similar comparisons for the flaps 15 configuration are shown in Fig. 16. The agreement between flight and computation is not as good at this condition as for the flaps 1 configuration. The higher lift levels achieved with this flap configuration result in greater viscous effects which the PAN AIR solutions have not simulated. The overall agreement between test and PAN AIR is still very good when the limitations of the computational theory and the geometrical complexity of the configuration have been accounted for.

A comparison of pressures measured on the nacelle with PAN AIR results are presented in Fig. 17. These comparisons are for the flaps 15 configuration and are quite similar to those observed at flaps 1. These comparisons show the large variation of pressure distribution around the nacelle at these high angle-of-attack conditions. The calculations were made at a nominal inlet mass flow ratio representative of engine operation at low-speed high angle-of-attack flight. No attempt was made to better match the exact engine mass flow ratio flown during the pressure measurements. In spite of a crude computational model for the nacelle, the agreement with experimental data is again quite good.

The results of these PAN AIR calculations as well as results from a multielement inviscid code based on two-dimensional PAN AIR technology with viscous and

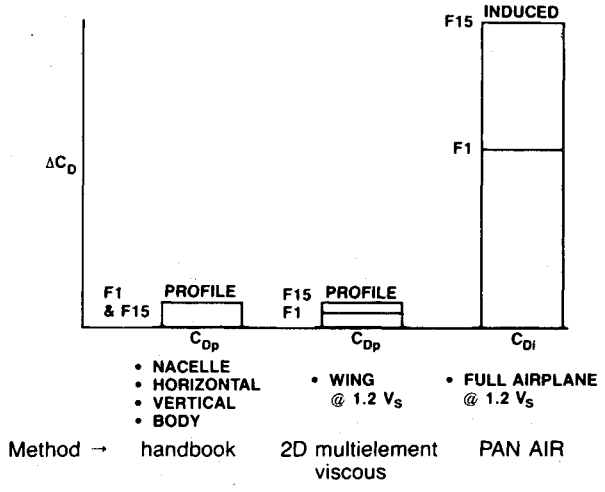

Fig. 18 Flaps down drag breakdown-takeoff flaps.

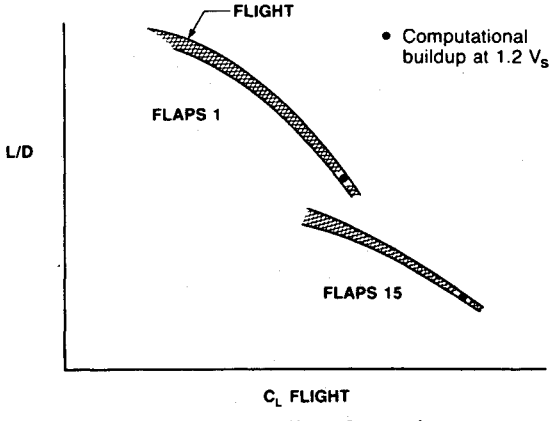

Fig. 19 Aircraft lift-to-drag ratio.

separated flow modeling,[12] a three-dimensional lifting surface multielement wing body code,[1] and handbook-type profile drag estimates were used to predict the aircraft L/D at the critical 1.2 V_{stall} condition. The drag buildups for both the flaps 1 and flaps 15 configurations are illustrated in Fig. 18. Handbook procedures were used to estimate the profile drag of all airplane components with exception of the wing. The wing profile drag was based on the spanwise integration of a series of two-dimensional analyses with the coupled inviscid/viscous modeling. The wing profile drag estimate had been made during the development of the 737-300 several years ago with the aid of the three-dimensional lifting surface multielement wing body code. The integrated surface pressures from the PAN AIR solutions were taken to represent the induced drag of the configuration. The advantage of using PAN AIR for this estimate is that it can adequately account for the presence of the engine nacelle, which in this aircraft is very large compared to the wing. The use of a higher order singularity distribution, the direct matrix solver, the splined pressure integration, and an adequately paneled model result in a high degree of accuracy in the calculation of induced drag on a complex configuration. The drag buildups were used to calculate aircraft L/D at the 1.2 V_{stall} condition. The comparison of the result of these buildups with performance data extracted from the precertification flights is shown in Fig. 19. The precertification performance data bands are 1–2% wide with the computed estimates falling within these bands.

The improved understanding of the flow details over the wing and nacelle, and of the drag build up at the critical 1.2 V_{stall} condition provided by the PAN AIR analysis aided in the development of the final FAA-certified configuration. Without a doubt, the final configuration could have been developed without the aid of the PAN AIR analysis, but whether it would have required one, two, or more additional development flights is not known. The key to the usefulness of the PAN AIR analysis was the timeliness of its availablility, unusual in that most CFD is done after the fact. Initial solutions were available within three weeks from the start of the analysis phase. Subsequent analyses were able to incorporate information gained during the flight development program such as the aeroelastic twist distribution and flap blow-back.

Concluding Remarks

PAN AIR panel method analyses of 737-300 takeoff high-lift configurations were performed in support of the aircraft's flight development phase during precertification flight test. The configurations analyzed featured a highly complex three-dimensional leading- and trailing-edge high-lift flap system. Modeling details of two takeoff flap settings consisting of significantly different flap and slat arrangements are presented. Computational results are presented and compared with flight test data. These comparisons include wing and nacelle pressure distributions, wing section lift coefficients, and aircraft L/D. The agreement of computational results with flight data is improved by incorporating inflight aeroelastic twist and flap blow-back into the model. These improvements to the geometric description of the computational model were based on in-flight optical measurements and 737 Structures Load staff estimates. The reliability and robustness of PAN AIR were important factors in its usability. Neither special modeling studies nor special care in panel or network ordering were necessary. Ensuring that all required network abutments were made and that panels did not intersect—conditions for which adequate program diagnostics are available—was required.

Acknowledgments

The authors would like to thank Messrs. Robert Rapp for providing some of the geometry and paneling for the aircraft, David J. Kotker for providing the flight pressure data, Michael L. Henderson for providing the drag buildups, and Mark O. Anderson for his help in analyzing the vast amount of computational results during the flight development phase of the program.

References

[1]Goldhammer, M. I., "A Lifting Surface Theory for the Analysis of Non-Planar Lifting Systems," AIAA Paper 76-18, Jan. 1976.

[2]Murillo, L. E. and McMasters, J. H., "A Method for Predicting Low-Speed Aerodynamic Characteristics of Transport Aircraft," *Journal of Aircraft*, Vol. 21, March 1984, pp. 168–174.

[3]Dillner, B., May, F. W., and McMasters, J. H., "Aerodynamic Issues in the Design of High-Lift Systems for Transport Aircraft," *Improvement of Aerodynamic Performance Through Boundary Layer Control and High-Lift Systems*, AGARD-CP-365, May 1984, pp. 9-1–9-22.

[4]Adair, W. A. and McRoberts, J. C., "Boeing 737-300 Flight Test Progress Report," AIAA Paper 84-2464, Nov. 1984.

[5]McRoberts, J. C., "Boeing 737-300 Flight Testing—The First Nine Months Service Experience," *29th Symposium Proceedings*, Society of Experimental Test Pilots, Beverly Hills, CA, Sept. 1985, pp. 51–66.

[6]Derbyshire, T. and Sidwell, K. W., "PAN AIR Summary Document, (Version 1.0)," NASA CR-3250, 1982.

[7]Magnus, A. E. and Epton, M. A., "PAN AIR—Computer Program for Predicting Subsonic or Supersonic Linear Potential Flows about Arbitrary Configurations Using a Higher Order Panel Method, Vol. 1, Theory Document (Version 1.0)," NASA CR-3251, 1980.

[8]Carmichael, R. L. and Erickson, L. L., "PAN AIR: A Higher Order Panel Method for Predicting Subsonic or Supersonic Linear Potential Flows about Arbitrary Configurations," AIAA Paper 81-1255, June 1981.

[9]Moran, J., Tinoco, E. N., and Johnson, F. T., "User's Manual—Subsonic/Supersonic Advanced Panel Pilot Code," NASA CR-152047, 1978.

[10]Chen, A. W. and Tinoco, E. N., "PAN AIR Applications to Aero-Propulsion Integration," *Journal of Aircraft*, Vol. 21, March 1984, pp. 161-167.

[11]Brune, G. W. and Hallstaff, T. H. "Wing Span Loads of Complex High-Lift Systems from Wake Measurements," *Journal of Aircraft*, Vol. 22, Sept. 1985, pp. 831-832.

[12]Henderson, M. L., "Two-Dimensional Separated Wake Modeling and Its Use to Predict Maximum Section Lift Coeficient," AIAA Paper 78-156, Jan. 1978.